THE ASTROPHYSICAL JOURNAL, 407:579–587, 1993 April 20

158 MICRON [C II] MAPPING OF NGC 6946: PROBING THE ATOMIC MEDIUM

S. C. MADDEN,[1] N. GEIS,[2] R. GENZEL,[1] F. HERRMANN,[1] J. JACKSON,[3] A. POGLITSCH,[1]
G. J. STACEY,[4] AND C. H. TOWNES[2]

Received 1992 April 13; accepted 1992 October 15

ABSTRACT

We present a well-sampled map of the strong 158 μm [C II] cooling line in the Scd galaxy NGC 6946 at 55″ resolution taken with the MPE/UCB Far-infrared Imaging Fabry-Perot Interferometer (FIFI) on the Kuiper Airborne Observatory (KAO). Significant far-infared line emission extends over an area of 8′ × 6′ (23 × 17 kpc) with a total luminosity of $3.0 \times 10^8\ L_\odot$, about 1% of the total far-infrared luminosity of the galaxy.

The [C II] emission comes from a mixture of components of interstellar gas. The brightest emission is associated with the nucleus, a second component traces the spiral arms and the largest star-forming/H II regions contained within them, and a third extended component of low brightness can be detected at least 12 kpc from the nucleus.

The nuclear and spiral arm components are most likely associated with dense ($n_H \geq 10^3$ cm^{-3}) photodissociation regions at molecular cloud surfaces that are exposed to ultraviolet radiation produced by young massive stars. We interpret the extended component as originating in the diffuse atomic (H I) medium of NGC 6946, representing the first detection of far-infrared line emission from atomic interstellar gas. The extended [C II] emission probably originates mainly in cold ($T \sim 100$ K), neutral hydrogen clouds having a pressure between 6.3×10^3 and 1.0×10^4 cm^{-3} K, similar to H I clouds in our Galaxy. We infer the volume filling factor of the cold H I clouds in NGC 6946 to be about 1%. Low-density H II regions can also contribute up to 50% of the extended [C II] emission. Hot ($T \sim 8000$ K) diffuse H I gas can only significantly contribute to the observed [C II] emission if it is clumped with a filling factor of less than 0.1 or has an ionization fraction exceeding 10%. The [C II] cooling rate in the atomic medium of NGC 6946 is $\sim 2 \times 10^{-25}$ ergs s^{-1} per hydrogen atom and is consistent with photoelectric heating by diffuse ultraviolet radiation.

Subject headings: galaxies: individual (NGC 6946) — galaxies: ISM — galaxies: spiral — infrared: galaxies

1. INTRODUCTION

Carbon, having an ionization potential of 11.3 eV, is the most abundant element in the interstellar medium with an ionization potential less than 13.6 eV. Since the $^2P_{3/2}$ fine-structure level of [C II] lies 91 K above the ground state and has a critical density of about 4×10^3 cm^{-3} in neutral hydrogen gas, the 157.7409 μm (Cooksy, Blake, & Saykally 1986) $^2P_{3/2} \rightarrow {}^2P_{1/2}$ [C II] fine-structure line is one of the most important cooling lines in neutral interstellar gas. Dalgarno & McCray (1972) predicted that the [C II] line is the dominant cooling line of the diffuse neutral atomic (H I) medium. The first detection of [C II] from Galactic sources indicated that the observed [C II] emission arises from fairly dense gas [$n(H) \sim 10^3$ cm^{-3}] associated with the surfaces of molecular clouds that are exposed to 912–2000 Å far-ultraviolet radiation (FUV) from embedded or external OB stars (Russell et al. 1981; Stacey et al. 1985; Crawford et al. 1985). The first observations of the [C II] line toward external galaxies, measured in the nuclei of gas-rich, luminous spirals, showed that the far-infrared line emission contributes up to 1% of the total luminosity (Crawford et al. 1985; Lugten et al. 1986; Stacey et al. 1991). The [C II] emission in these extragalactic nuclei likely originates in moderately dense photodissociation regions (PDRs) near star formation regions at the edges of molecular clouds (Tielens & Hollenbach 1985; Wolfire, Hollenbach, & Tielens 1990).

With the recent availability of the Max-Planck-Institut für extraterrestrische Physik (MPE)–University of California, Berkeley (UCB) Far-infrared Imaging Fabry-Perot Interferometer (FIFI) (Poglitsch et al. 1990, 1991; Stacey et al. 1992), it is now possible to study the spatial distribution and physical properties of far-infrared line emission in the disks of external galaxies. We report here the first large-scale image of [C II] 158 μm emission in the gas-rich Scd galaxy NGC 6946. NGC 6946 is a low-inclination ($i = 34°$), multiarmed galaxy with evidence for a spiral density wave. It has been investigated in detail in the radio continuum (van der Kruit, Allen, & Rots 1977; Klein & Emerson 1981; Klein et al. 1982), the H I 21 cm line (Tacconi & Young 1986; Carignan et al. 1990), CO rotational lines (Ball et al. 1985; Weliachew, Casoli, & Combes 1988; Sofue et al. 1988; Tacconi & Young 1989; Casoli et al. 1990; Wild 1990; Ishizuki et al. 1990), the far-infrared continuum (Smith, Harper, & Loewenstein 1984; Engargiola 1991), and in Hα (DeGioia-Eastwood et al. 1984; Bonnarel, Boulesteix, & Marcelin 1986). Previous [C II] observations in the nuclear region of NGC 6946 are presented by Stacey et al. (1991) with preliminary mapping of the central 3′ × 3′ region by Geis (1991) and Stacey et al. (1990). Although the distance is uncertain, we adopt a distance of 10.1 Mpc (Rogstad, Shostak, & Rots 1973; Sandage & Tammann 1974). At this distance, 1′ corresponds to 2.9 kpc.

[1] Max-Planck-Institut für extraterrestrische Physik, Gießenbachstraße, D-8046 Garching bei München, Germany.
[2] Department of Physics, University of California, Berkeley, CA 94720.
[3] Department of Astronomy, Boston University, Boston, MA 02215.
[4] Department of Astronomy, Cornell University, Ithaca, NY 14853-6801.

2. OBSERVATIONS

We observed the [C II] 157.7409 μm line toward NGC 6946 with the Kuiper Airborne Observatory (KAO) on flights from Moffett Field, California in 1990 September and October and in 1991 September. Full descriptions of FIFI are in Poglitsch et al. (1990, 1991) and Stacey et al. (1992). The spatial response function of each pixel in the 5 × 5 detector array approximates a 55″ (FWHM) Gaussian (68″ equivalent disk with a corresponding beam solid angle of 8.3×10^{-8} sr). Detectors are separated on the sky by 40″, and a K-mirror compensates for sky rotation of the image to maintain orientation of the rectangular array on the sky. The observations were made with 80 km s^{-1} spectral resolution. The 25 stressed Ge:Ga detectors (Stacey et al. 1992) had system noise-equivalent powers (NEPs) ranging between 5 and 14×10^{-15} W Hz$^{-1/2}$, including all telescope, instrument, and atmospheric losses. Observations were taken by chopping the telescope's secondary 6′ in declination at 23 Hz. The telescope nodded to compensate for differential offsets between beams.

Data were obtained toward eight separate center positions for the detector array, resulting in a half-beam spacing map of the [C II] emission with 162 independent spatial points over an 8′ × 6′ area on the sky. Data in the central part of NGC 6946, where there is a sizeable velocity gradient, were taken by scanning four or five spectral resolution elements across the line; the line flux was determined by setting a baseline and integrating. The outer parts of NGC 6946, where the velocity gradients are small and the continuum levels low, were observed by fixing the Fabry-Perot at the velocities appropriate for the two sides of the galaxy: −20 km s^{-1} east and +120 km s^{-1} west with respect to the velocity of the nucleus. The 160 μm continuum map of Engargiola (1991) indicates that the continuum is less than 10% of the line fluxes in our bandwidth, so we ignore possible 158 μm continuum contamination of our observed line fluxes. Flat-fielding was performed with internal hot and cold blackbody loads of known temperatures. The measurements required a total integration time on the source of 4.0 hr.

Where several measurements were available for the same position (which is the case for about half of the data points), individual measurements were weighted by noise and averaged. Absolute line intensities were calibrated by observing Orion KL and are estimated to be accurate to ±30%. Absolute positions are uncertain by ∼15″. Our measured nuclear [C II] intensity, 7×10^{-5} ergs s^{-1} cm^{-2} sr^{-1}, compares well with the value of Stacey et al. (1991), taken with a different spectrometer but the same beam size.

3. RESULTS

3.1. *Spatial Distribution of the* [C II] *Emission: Three Components*

The [C II] map is shown in Figure 1*a* (Plates 12 and 13) superposed on an optical image of NGC 6946. We find significant [C II] emission over most of the region mapped (8′ × 6′). The signal-to-noise ratio of individual data points is typically 5 to 10. Some negative intensities in the northeast and southwest positions indicate that the [C II] emission is more extended than our chopper throw of 6′. Negative intensities are caused by emission in the reference beams ("self-chopping") or imperfect cancellation of the telescope offset.

Based on simple morphological considerations, we decompose the [C II] emission of Figure 1*a* into three spatially distinct components: nucleus, spiral arms, and extended region. The brightest [C II] emission comes from the nucleus (FWHM size R.A. × Decl. ≈ 1.′3 × 2.′5). In the component associated with the spiral arms, local peaks of [C II] emission are seen on or near the most prominent star formation/H II regions within the arms (e.g., the Hα of Bonnarel et al. 1986). Despite differences in resolution, the similarity between the [C II] and optical images in Figure 1*a* suggests a close connection between the nuclear and spiral arm [C II] components and the optical continuum/Hα that traces the current massive star formation activity. A third component of extended and weaker [C II] emission, not obviously connected with optical emission and star formation activity, is detected out to a radius of 4′ (12 kpc). This component is especially obvious in the region 3′–4′ west of the nucleus and in the region about 3′ to the southeast where the optical emission is faint.

3.2. *Comparison of* [C II] *with Other Tracers*

As east-west cut through the nucleus of the various tracers [C II], FIR, CO, and H I taken with similar beam sizes is displayed in Figure 2. The cut extends through one of the prominent eastern spiral arms 2.′2–2.′5 east of the nucleus and a second, somewhat fainter arm 2′ west of the nucleus. The spiral arms are seen most easily from this cut in the [C II] and not very obvious at this resolution (45″) in the CO and FIR. The CO and FIR continuum and [C II] emission are strongly peaked toward the nucleus, in contrast to H I which shows a minimum toward the nucleus. [C II] clearly shows an extended emission component further out in the disk where the H I peaks and where CO and FIR emission is faint.

3.2.1. *Comparison with FIR Continuum*

The far-infrared continuum and [C II] peaks coincide remarkably well throughout NGC 6946 (Fig. 1*b*). In addition to the spatial agreement between the prominent [C II] and 160 μm maxima in the nucleus, there is excellent agreement of the locations of secondary [C II] peaks with discrete sources of 160 μm continuum emission (Engargiola 1991). The 160 μm obser-

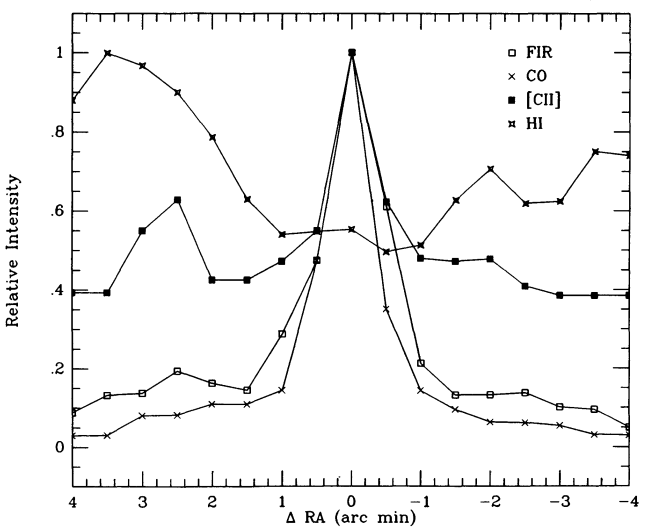

FIG. 2.—Cut in NGC 6946 in R.A. from east to west along Δdecl. = 0 in the various tracers: H I (*open star*), [C II] (*filled square*), 160 μm (*open square*), and CO (*cross*). Data are from Fig. 1.

PLATE 12

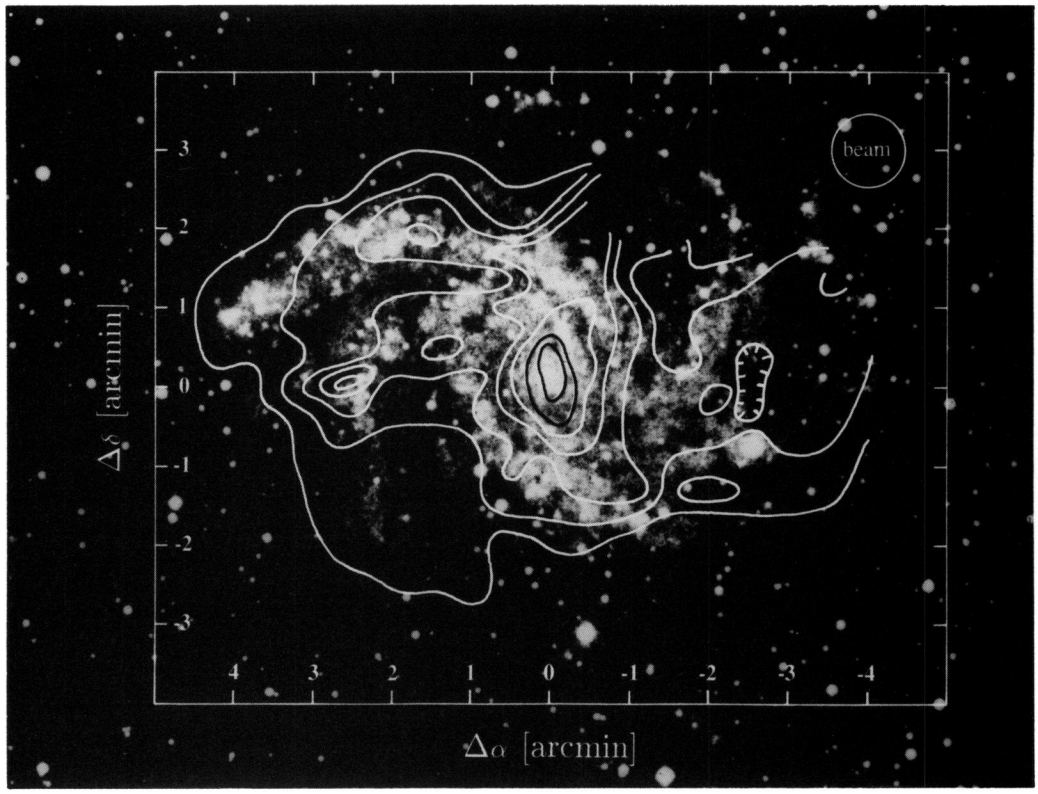

FIG. 1a

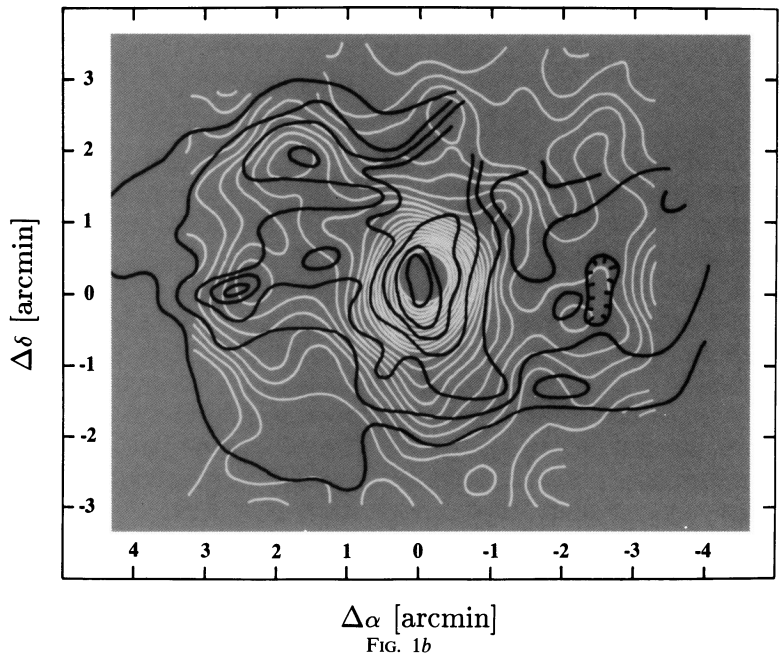

FIG. 1b

FIG. 1.—Integrated [C II] line intensity contours (*black*) with contour interval of 1 × 10^{-5} ergs s^{-1} cm^{-2} sr^{-1} and peak value of 7 × 10^{-5} ergs s^{-1} cm^{-2} sr^{-1} superposed on (*a*) an optical image of NGC 6946, (*b*) 160 μm contours with a spacing of 2 Jy $beam^{-1}$ and peak of 57 Jy $beam^{-1}$ (Engargiola 1991), (*c*) CO contours (*white*) which range from 2 to 44 K km s^{-1} in intervals of 3 K km s^{-1} (Tacconi & Young 1989), and (*d*) H I contours (*white*) of intervals 0.3 Jy km s^{-1} with extremes of 0.3 and 3.3 Jy km s^{-1} (Tacconi & Young 1989). The center position is R.A.(1950) $20^h33^m48^s.8$, decl.(1950) +59°58′50″.

MADDEN et al. (see 407, 580)

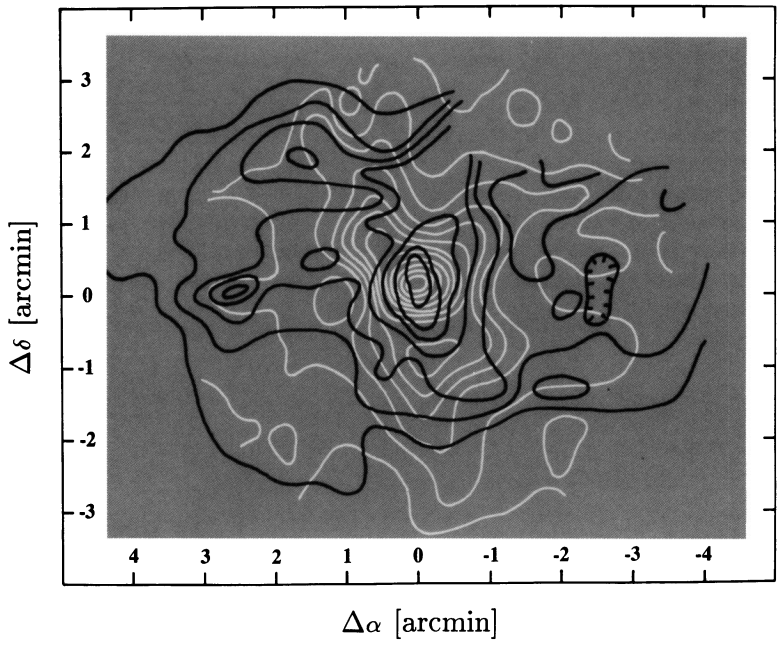

FIG. 1*c*

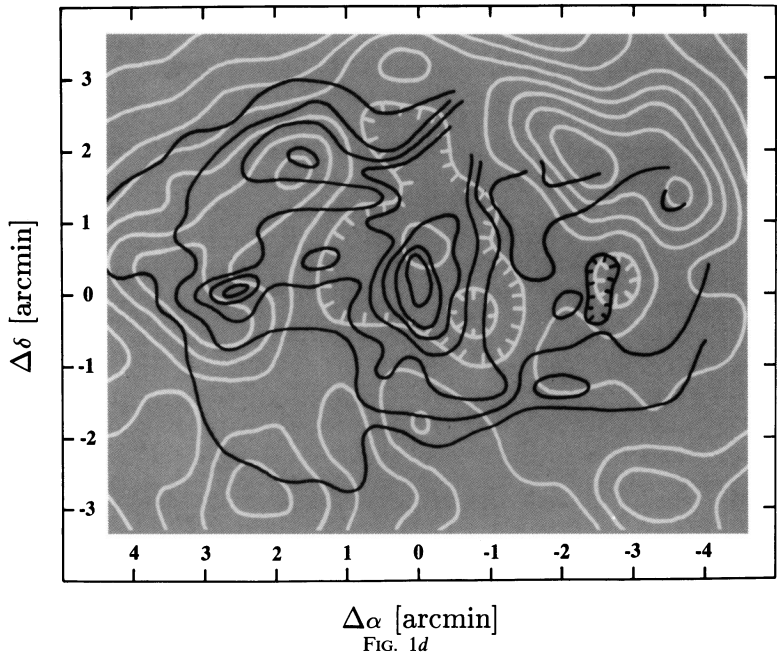

FIG. 1*d*

MADDEN et al. (see 407, 580)

vations were made with a 45″ aperture, suitable for direct comparison with the [C II] data.

3.2.2. *Comparison with Molecular Gas*

[C II] and CO (45″ beam; Tacconi & Young 1989) agree fairly well in the central part of NGC 6946 (Fig. 1*c*). The [C II] and CO peaks coincide in the nucleus, and both tracers have extensions to the northeast, in the direction of the brightest spiral arm in the galaxy. The molecular cloud concentrations in the eastern and northeastern spiral arm structures seen in the higher resolution CO (1–0) and CO (2–1) observations (Casoli et al. 1990; Tacconi, Tacconi-Garman, & Xie 1993) coincide with the local spiral arm peaks in the [C II] data. The north-south elongation seen in [C II] in the nucleus is suggestive of the molecular bar structure revealed in the higher resolution CO observations of the nuclear region (Ball et al. 1985; Sofue et al. 1988; Weliachew et al. 1988; Ishizuki et al. 1990).

3.2.3. *Comparison with Atomic Gas*

The extended [C II] distribution in the outer part of NGC 6946 resembles the H I distribution. H I data have been taken with a 21″ synthesized beam and convolved to 55″ for direct comparison with our [C II] data (Fig. 1*d*; L. Tacconi 1992, private communication). The H I emission drops in the center, where the [C II] peaks. The northeastern and eastern spiral arm, and perhaps the western arm as seen in [C II], coincide with features in the H I ring. Several local maxima present in H I are on or near the secondary [C II] peaks.

3.3. *Mass and Luminosity of the* [C II] *Components*

We estimate that the nuclear component has a peak [C II] brightness of 5–6 $\times$ 10^{-5} ergs s^{-1} cm^{-2} sr^{-1} in the central 1′, contributing a line luminosity of 1.5 $\times$ 10^7 $L_\odot$. The nuclear ridge (central 1.′3 $\times$ 2.′5) and the spiral arm component (including four spiral arms each of average area 2′ $\times$ 1′) each contribute 5 $\times$ 10^7 $L_\odot$. The extended [C II] component (8′ $\times$ 6′) has a [C II] intensity ranging from 1 to 2 $\times$ 10^{-5} ergs s^{-1} cm^{-2} sr^{-1} and contains a line luminosity of $\sim$2.0 $\times$ 10^8 $L_\odot$. The total [C II] luminosity within 12 kpc of the nucleus of NGC 6946 is about 2.6 $\times$ 10^8 $L_\odot$ (nucleus, spiral arms, and extended component) with at least 70% contributed by the extended component. The [C II] line thus contributes 0.2% to the 12–200 μm far-infrared continuum luminosity of the central 1′ [$L_{FIR}(1') = 8 \times 10^9$ $L_\odot$; Engargiola 1991] and approximately 1% to the luminosity of the central 8′ $\times$ 6′ (L_{FIR} = 2.5 $\times$ 10^{10} $L_\odot$). These findings agree well with the results of Stacey et al. (1991) who found that the [C II] accounts for 0.1%–1% of the far-infrared luminosity in the nuclear regions in a sample of 14 galaxies. Similarly, measurements of the Galactic [C II] emission (Stacey et al. 1985; Stacey 1985; Shibai et al. 1991; Wright et al. 1991) show that the [C II] line emission accounts for approximately 0.3% of the far-infrared continuum in the inner Galaxy. For comparison, Table 1 contains [C II] and FIR luminosities of previously measured starburst and "quiescent" nuclei.

The [C II]–emitting regions may contain a significant fraction of interstellar gas in the galaxy (Crawford et al. 1985; Stacey et al. 1991). The column density of hydrogenic nuclei, $N_{C^+}(H)$, associated with the [C II] emission is (Crawford et al. 1985)

$$N_{C^+}(H) = 4.25 \times 10^{20} \left[\frac{1 + 2\exp(-91.3/T) + (n_{crit}/n_H)}{2\exp(-91.3/T)}\right] \frac{I_{C^+}}{X_{C^+}} . \quad (1)$$

The fractional abundance of carbon is $X_{C^+} = [C^+]/[H]$, the kinetic temperature T is in kelvins, I_{C^+} is the [C II] line brightness in ergs s^{-1} cm^{-2} sr^{-1}, and n_H is the local hydrogen particle density. A lower limit to the column density of hydrogenic nuclei associated with the [C II] emission, $N_{min}(H)$, and mass inferred from this column density, $M_{C^+}^{min}(H)$, can be estimated by assuming that n_H is much larger than the critical density of the $J = 3/2$ state ($n_{crit} \sim 4 \times 10^3$ cm^{-3}; Launay & Roueff 1977; Flower & Launay 1977), and temperatures are much larger than $h\nu/k$ = 91.3 K, the energy of the $^2P_{3/2}$ state above ground:

$$N_{C^+}^{min}(H) = 2.1 \times 10^{24} I_{C^+} ,$$
$$M_{C^+}^{min} = 7.8 \times 10^7 [N_{C^+}^{min}(H)/10^{21}\ cm^{-2}] \theta^2 D_{10.1}^2 . \quad (2)$$

$N_{C^+}^{min}(H)$ is given in units of cm^{-2}, $M_{C^+}^{min}$ is in $M_\odot$, I_{C^+} is in units of ergs s^{-1} cm^{-2} sr^{-1}, θ (in arcmin) is the FWHM size of the source with assumed Gaussian shape and $D_{10.1}$ is the distance of NGC 6946 in units of 10.1 Mpc. We have assumed all carbon is in the form C^+, giving $X_{C^+} = 3 \times 10^{-4}$. The minimum hydrogen masses in the [C II]–emitting regions associated with the nuclear, spiral arm, and extended [C II] components are then 3, 3, and 10 $\times$ 10^7 $M_\odot$, respectively.

TABLE 1

COMPARISON OF RELATIVE MASSES AND LUMINOSITIES OF DIFFERENT COMPONENTS IN NGC 6946 AND OTHER GALAXIES

Galaxy	$M(H_2)$[a] ($M_\odot$)	M(H I)[b] ($M_\odot$)	$M_{C^+}^{min}$(H)[c] ($M_\odot$)	$L_{[CII]}$ ($\times 10^7$ $L_\odot$)	L_{FIR} ($\times 10^9$ $L_\odot$)
NGC 6946 nucleus (Central 1′)	180	6	1	1.5	8.0[e]
NGC 6946 spiral arm (eastern spiral arm, ΔR.A. = +150″)	33	7	1	5.0	5.5[e]
NGC 6946 extended component	$\leq$20	30	1	20.0	0.7[e]
Starburst nuclei[d] (Central 1′ of M82, IC 342, and M83)	3–20	1	1	0.3–5.0	0.6–28.0
"Quiescent" nuclei[d] (NGC 891 and NGC 3079)	30–150	10	1	3.0–8.0	9.0–28.0

[a] Derived from the CO(1–0) data of Tacconi & Young 1989, Weliachew et al. 1987, Casoli et al. 1990, and Wild 1991.
[b] H I mass determined from H I observations: Tacconi & Young 1986 and Carignan et al. 1990.
[c] Minimum hydrogen mass in [C II] emission zone (see § 3.3).
[d] From Stacey et al. 1991.
[e] From Engargiola 1991.

Note that the high-temperature, high-density approximations that are assumed to obtain the minimum masses here are typical conditions for molecular cloud surfaces that are exposed to photodissociating radiation (PDRs; § 4.1). Relaxing these conditions would give higher mass estimates in the [C II]–emitting gas.

Estimates of the column densities and masses of the molecular and atomic tracers in these three components of NGC 6946 may be derived using CO (1–0) of Tacconi & Young (1989) and Carignan et al. (1990) and H I from Tacconi & Young (1986). We use the standard relationships between velocity-integrated CO (1–0) intensity, $I_{CO} = \int T_B(\mathrm{CO})dv$ [K km s^{-1}] or H I intensity $I_{HI} = \int T_B(\mathrm{H\ I})dv$ [K km s^{-1}] (T_B is the line brightness temperature), and hydrogen column density (e.g., Bloemen 1989; Kulkarni & Heiles 1988):

$$2N(\mathrm{H_2}) \sim 4 \times 10^{20} I_{\mathrm{CO}\,(1-0)} \quad (3)$$

and

$$N(\mathrm{H\ I}) = 1.83 \times 10^{18} I_{\mathrm{H\,I}}\,. \quad (4)$$

Table 1 lists the *relative* masses for the CO–, H I–, and [C II]–emitting gas for the components of NGC 6946, along with those of typical starburst nuclei (M82, IC 342, M83) and of normal, nonstarburst spiral galaxy nuclei (NGC 891, NGC 3079; Stacey et al. 1991). Starburst galaxies have about the same mass fraction of interstellar gas in the [C II]–emitting gas and the atomic medium. Typically, the minimum mass in each of these components is ~10% of the gas in molecular gas, as estimated from the standard CO intensity to mass conversion factor. In contrast, quiescent nuclei tend to have a much smaller mass fraction in [C II]–emitting gas (~few percent; Stacey et al. 1991).

According to these criteria NGC 6946 is a good example of a normal, quiescent nucleus, while the spiral arm peaks range between the characteristics of quiescent and starburst. The extended emission component in NGC 6946, however, does not fall into either of these two categories. Here the mass in atomic hydrogen is at least as large as that in molecular gas.

4. ORIGIN OF THE [C II] LINE

Spatial information allows us to separate different components of the [C II] emission in NGC 6946 and determine the origin of the [C II] intensity. Possible origins of the extended, spiral arm, and nuclear components of the [C II] emission in NGC 6946 are the H I gas, H II regions, and photodissociation regions.

4.1. *Photodissociation Regions*

Neutral material at the edges of molecular or atomic clouds can be ionized or dissociated by UV radiation from photons longward of the Lyman limit, $\lambda \geq 912$ Å (≤ 13.6 eV) originating from nearby O and B stars. Warm interface regions between molecular clouds and H II regions called photodissociation regions (PDRs) are formed. The CO (1–0) line becomes optically thick near the UV exposed layers, and the far-infrared dust continuum is produced by thermal reradiation of the absorbed UV photons. If we assume that [C II] and CO line emission as well as the far-infrared continuum all originate at the surfaces of the UV-exposed molecular clouds, then the beam filling factor of all of these three tracers is about the same. The ratios of [C II] to far-infrared continuum intensities (Y_{C^+}) and of CO to far-infrared continuum intensities (Y_{CO}) are then independent of filling factor and may be used in conjunction with PDR models to derive the physical conditions of the emitting cloud (Wolfire et al. 1990). We present an analysis of the [C II] observations in NGC 6946 in terms of these PDR models since the spatial coincidence with CO, FIR continuum, and star formation regions in much of NGC 6946 suggests that PDRs are an obvious origin. [C II] emission in various Galactic and extragalactic sources has also been successfully interpreted as arising in PDRs of molecular cloud surfaces (cf. Genzel, Harris, & Stutzki 1989; Stacey 1989; Wolfire et al. 1990; Stacey et al. 1991).

Table 2 lists the observed and derived parameters of this PDR analysis for the three emission regions in NGC 6946 following the work of Stacey et al. (1991) who also give a detailed description of the PDR parameters. A constant value for the [C II] intensity has been assumed for the extended component and subtracted from the total [C II] intensities for the spiral arm and nuclear components. The PDR solutions for UV field strengths and n_H as functions of the observed parameters, Y_{C^+} and Y_{CO}, are shown in Figure 3. As seen from Figure 3 the PDR solutions are double valued. The higher density solutions for the components require UV field intensities (χ_{UV}) ranging from 400 to 2×10^3 times χ_0, the UV field in the solar neighborhood (2.0×10^{-4} ergs s^{-1} cm^{-2} sr^{-1}; Draine 1978), and hydrogen volume densities which are characteristic of dense ($n_H > 10^4$ cm^{-3}) interstellar clouds, while the lower

TABLE 2

PDR MODEL RESULTS OF THE [C II] EMISSION IN NGC 6946[a]

NGC 6946 COMPONENT	OBSERVATIONS			MODEL OUTPUT		
	χ_{FIR}/χ_0	Y_{C^+}[b] ($\times 10^{-6}$)	Y_{CO}[b] ($\times 10^{-10}$)	χ_{UV}/χ_0	n(H)	Φ_{FIR}[e]
Nucleus	120	0.5	10	400	8×10^5[c]	0.15
				<100	<100	>0.6
Spiral arm peaks	43	0.6	2.3	2×10^3	2×10^5[c]	0.01
				320	3×10^2[d]	0.07
Extended component	12	1.3	3.5	600	2×10^4[c]	0.01
				300	1×10^3[d]	0.02

[a] For the 55″ [C II] beam after decomposition of the data into three components.
[b] $Y_{C^+} = I_{C^+}/(\chi_{FIR}/\chi_0)$; $Y_{CO} = I_{CO}\,1.55 \times 10^{-9}/(\chi_{FIR}/\chi_0)$.
[c] High-density solution.
[d] Low-density solution.
[e] $\Phi = (\chi_{FIR}/2)/\chi_{UV}$, the area filling factor of UV radiation.

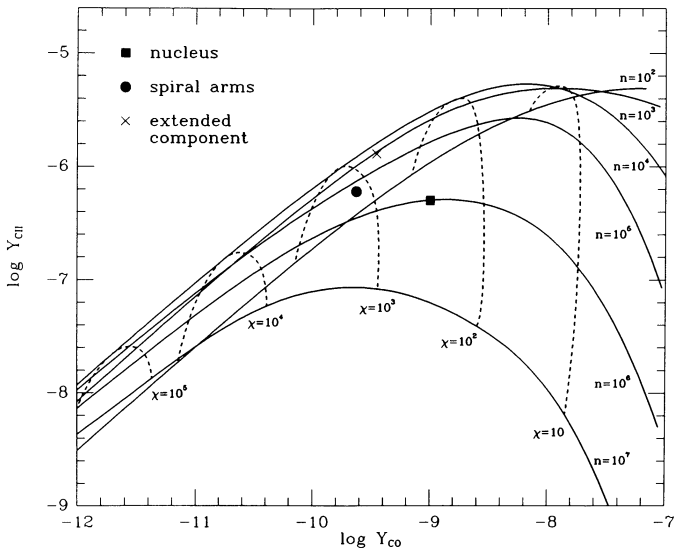

FIG. 3.—Lines of constant density (n) and χ_{UV} (χ) are shown as PDR solutions for $Y_{C^+}(I_{C^+}/[\chi_{FIR}/\chi_0])$ vs. $Y_{CO}(I_{CO}/[\chi_{FIR}/\chi_0])$. Solutions for the nuclear component (*cross*), spiral arms (*filled circle*), and extended component (*filled square*) of NGC 6946 are indicated.

density solutions give n_H ranging from less than 100–10^3 cm^{-3} with UV fields less than 100–300 times χ_0 (Fig. 3, Table 2).

In the PDR models the ratio of the "observed" UV fluxes (assuming $\chi_{FIR} \sim 2\chi_{UV}$[observed] Wolfire et al. 1990), to the "theoretical" UV fluxes from PDR models (χ_{UV}[theoretical]), is an estimate of the area filling factor, Φ (Table 2). The area filling factor of the nuclear source, based on the higher density solution, is 0.15 in our 55″ beam. This corresponds to a 20″ diameter Gaussian source, in fairly good agreement with the diameter of the nuclear source when observed at high spatial resolution in Hα (Bonnarel et al. 1986) or CO (Ball et al. 1985; Weliachew et al. 1988; Wild 1991). The low-density solution is less likely in the nucleus since in this case the requirements would give densities less than 100 cm^{-3} and UV field strengths lower than χ_{FIR} giving an area filling factor greater than 0.6. The inferred equivalent sizes of the spiral arm peaks are 7″ or 14″ (for the high- or low-density solutions, respectively)—also consistent with high-resolution Hα and CO data which indicate sizes for the most prominent cloud/H II region complexes of 10″ × 20″.

In the extended [C II] component, the [C II] line to far-infrared continuum ratio is large, while the ratio of CO to far-infrared continuum is not. If our observed [C II] intensity in the extended component originates from PDRs, it follows from the PDR models that both the density (10^3–10^4 cm^{-3}) and the UV flux (300–600χ_0) must be high. The area filling factors of the sources in the extended component are then inferred to be very small, corresponding to sizes of about 5″–7″. With the required high densities and high-UV fields, these would necessarily be OB star-forming regions and their associated molecular clouds. It seems implausible that the [C II] component is spatially extended over 10 kpc on large scales and at the same time clumped into many small high-density clouds. The radiation field would have to be clumped on similar size scales, and we see no evidence for this in other tracers, for instance, as individual star-forming complexes seen on high-resolution Hα maps (DeGoia-Eastwood et al. 1984). We conclude that the standard PDR models, which assume complete conversion to molecular gas, do not account for the [C II] emission in the extended component.

We could also postulate a situation where our source is fragmented into very small clouds producing, for example, large [C II] halos surrounding very small molecular cores. This would result in differing [C II] and CO filling factors thus rendering the essential assumption of similar beam filling factors for the PDR models inappropriate. However, this then would be more representative of the atomic medium which we consider next.

4.2. *The Extended* [C II] *Component: Atomic Gas*

The [C II] in the extended component is associated with a relatively large mass ($\sim 10^8\ M_\odot$). Since the H I column density is high beyond the spiral arms, in contrast to the molecular gas, we consider the excitation of [C II] from the atomic gas. The diffuse atomic component of the interstellar medium in our own Galaxy is thought to be composed of a cold neutral medium (CNM) with a temperature of about 80 K, a warm neutral medium (WNM) of about 8000 K, and a warm ionized medium (WIM) of 8000 K, all postulated to be in rough pressure equilibrium (Kulkarni & Heiles 1987; Kulkarni & Heiles 1988; Heiles 1988). Cooling in the diffuse ISM is primarily due to [C II] 158 μm line emission following collisional excitation of the $^2P_{3/2}$ level of [C II] by neutral hydrogen atoms and electrons (Dalgarno & McCray 1977; Stacey 1985). The critical density for collisions with electrons in 8000 K gas is $\sim$35 cm^{-3}, while collisions with H I have critical densities of $\sim 2 \times 10^3$ cm^{-3} for 300 K gas (Launay & Roueff 1977; Hayes & Nussbaumer 1984). The relative importance of these processes depends on the fractional ionization [$X_e = (e)/(\mathrm{H})$], with electron impact excitation dominant for X_e greater than about 10^{-3} (Dalgarno & McCray 1972). In the neutral regions, in addition to the ionization contribution from heavy elements, cosmic-ray ionization of H I contributes substantially to the number of free electrons. In our own Galaxy, X_e is estimated to be within a factor of 3 of $\sim 6 \times 10^{-4}$ in the CNM and $\sim 3 \times 10^{-2}$ in the WNM (Kulkarni & Heiles 1987; Heiles 1988). We investigate the excitation of our observed [C II] in the extended component of NGC 6946 including both impact mechanisms in the following expression, expanded from equation (1):

$$I_{C^+}(\mathrm{H}+e) = 2.35 \times 10^{-21} \times \left\{ \frac{2\exp(-91.3/T)}{1+2\exp(-91.3/T)+[n_{crit}(\mathrm{H})/n_H]} + \frac{2\exp(-91.3/T)}{1+2\exp(-91.3/T)+[n_{crit}(e)/n_e]} \right\} X_{C^+} N(\mathrm{H\ I}). \quad (5)$$

The hydrogen and electron densities, n_H and n_e, are in units of cm^{-3} and $n_e = n_H X_e$. N(H I) is the observed column density of H I in cm^{-3}, and I_{C^+}(H I + e) is the 158 μm [C II] intensity observed in the extended component ($\sim 1.5 \times 10^{-5}$ ergs s^{-1} cm^{-2} sr^{-1}) assumed to be excited by H I and electron collisions. The observed $I_{H\,I}$ integrated intensity of 700 K km s^{-1}, averaged over the extended [C II] disk region, gives $N(\mathrm{H\ I}) \approx 1.1 \times 10^{21}$ cm^{-2} (Tacconi & Young 1986; Carignan et al. 1990). The critical densities for collisions with H I [n_{crit}(H)] and electrons [$n_{crit}(e)$] were fitted as functions of temperature from the calculations of Launay & Roueff (1977) and

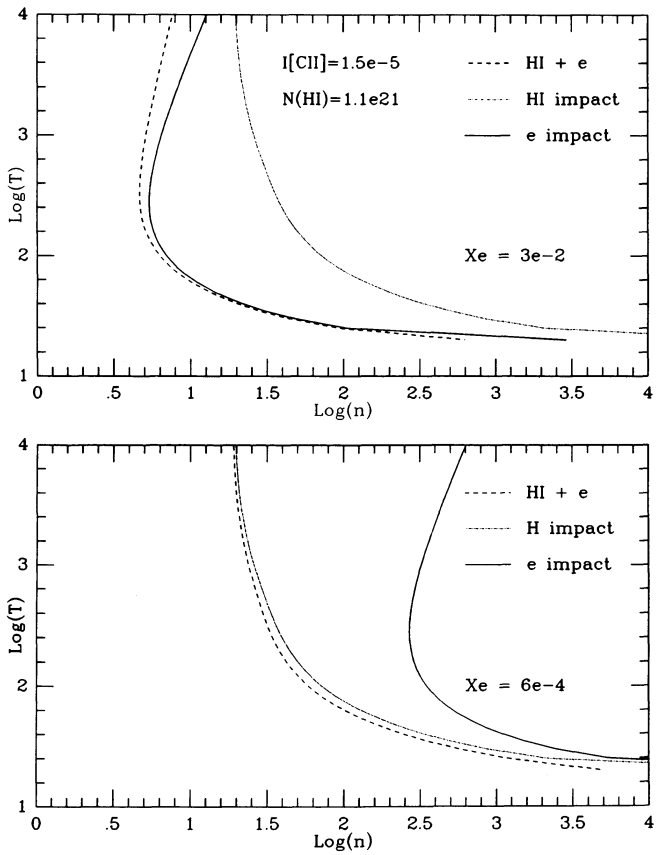

FIG. 4.—Temperature-density solutions for the extended component of the observed [C II] intensity and H I column density for collisions with H I only (*dotted*), electrons only (*solid*), and both (*dashed*) in the neutral atomic medium. Panel *a* uses fractional ionization (X_e) = 0.03, representative of the warm neutral medium (WNM), and panel *b* uses $X_e = 6 \times 10^{-4}$ for the cold neutral medium (CNM). The solutions which include both H I and the electron impact processes (*dashed lines*) mostly involve electron collisions for the WNM (*a*) and H I collisions for the CNM (*b*), as expected.

Hayes & Nussbaumer (1984). Figure 4 shows possible temperature and density solutions for the postulated WNM and CNM in the extended disk of NGC 6946. Solutions considering both electron and H I impact excitation together are shown as well as the cases if only one or the other process were in effect. Electron impact excitation dominates the higher fractional ionization case (Fig. 4*a*) as expected, while in the lower electron abundance medium (Fig. 4*b*) collisions are dominated by H I. For these solutions we have used the observed values of the [C II] intensity and the H I column density to solve equation (5).

4.2.1. *Cold* H I *Clouds*

If we assume that the atomic clouds in NGC 6946 have about the same kinetic temperature, $T_{KIN} \sim 80$ K, in the CNM (Kulkari & Heiles 1987, 1988) derived from the H I observations in our Galaxy, we find $n \sim 90$ cm^{-3} (Fig. 4). For this case where X_e is expected to be 6×10^{-4}, we see from Figure 4 that electron impact excitation is not important in the low-density regime of interest for the CNM. If we include the full possible range of temperatures, 40–400 K, deduced for the CNM in our galaxy (Kulkarni & Heiles 1987), we find a similarly wide spread of allowable densities (25–250 cm^{-3}), but the pressure of the CNM is well constrained between 6.3×10^3 cm^{-3} K, the minimum value, and 1.0×10^4 cm^{-3} K (Fig. 5). This pressure is consistent with the value of 8000 cm^{-3} K derived for the diffuse local interstellar medium of our Galaxy from ultraviolet C^0 measurements (Pottasch, Wesselius, & van Duinen 1979). Ultraviolet C^+ measurements give a range of pressures of 10^3–10^4 cm^{-3} K with a median value of 4000 cm^{-3} K (Jenkins, Jura, & Lowenstein 1983). We have assumed solar carbon abundance with no significant depletion of carbon onto grains in our analysis. Assuming depletion would result in a higher pressure for this medium.

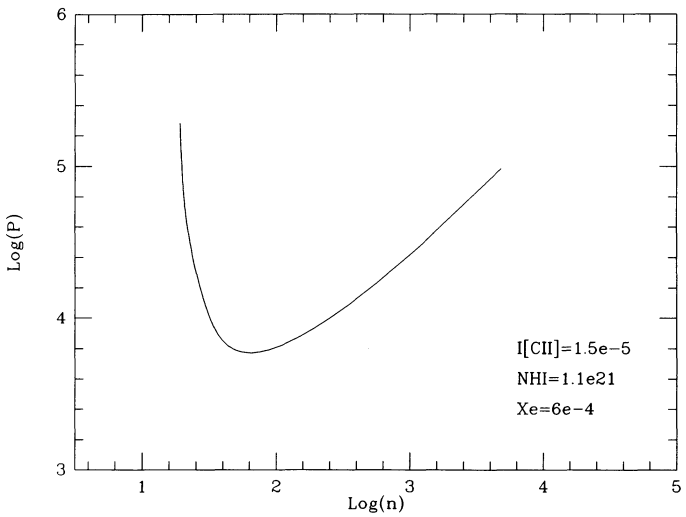

FIG. 5.—Pressure solutions for the observed [C II] intensity and H I column density in the extended component of NGC 6946 in the cold neutral medium. If all of the [C II] arises from the CNM, the pressure can range from 6000 to 10,000 cm^{-3} K (see § 4.2.1).

Assuming an H I full width at half-maximum (FWHM) of 230 pc, as in our Galaxy (Kulkarni & Heiles 1987; Dickey & Lockman 1990), we derive an average hydrogen density in the extended disk of NGC 6946 of $\langle n(\mathrm{H})\rangle = N(\mathrm{H\ I}) \cos(i)/\mathrm{FWHM} = 1.3$ cm^{-3} and a volume filling factor of the H I medium of $\Phi_v = \langle n(\mathrm{H})\rangle / n(\mathrm{H}) \sim 0.005$ to 0.05 for $n = 25$–250 cm^{-3}. Clumpy cold atomic clouds, therefore, can explain the observed [C II] extended emission in NGC 6946. In the Galaxy, the CNM is also thought to be organized in discrete clouds (see Kulkarni & Heiles 1987), consistent with our results for the CNM in NGC 6946.

4.2.2. *Warm Diffuse* H I

If the [C II] intensity originates from a WNM, the excitation is dominated by electron impacts (Fig. 4) assuming the fractional ionization is greater than or about equal to 0.03, the value estimated for the WNM in our Galaxy (Kulkarni & Heiles 1988). Assuming temperatures identical to those of the WNM of our Galaxy 4000–8000 K (e.g., Kulkarni & Heiles 1987), we find $n_H \sim 7$ cm^{-3} to account for the [C II] in NGC 6946. Using a FWHM $\sim$ 500 pc deduced for the WNM in the Galaxy (Kulkarni & Heiles 1987), the mean density is about 0.6 cm^{-3} assuming all of the H I is in the WNM. Unless the filling factor of the warm diffuse medium is <0.1, the WNM cannot explain a large fraction of the [C II] intensity if the scale height is similar to our Galaxy. This small filling factor is not consistent with the picture formulated for the Galaxy: the WNM is thought to fill much of the space between the discrete cold atomic clouds with a postulated filling factor of about 30% (Kulkarni & Heiles 1987). In this analysis, we are attributing

all of the observed H I to the WNM. If some smaller fraction of the H I arises from the WNM (more likely), then the filling factors calculated above would be even smaller. However, if we only reduce the scale height of the warm diffuse medium by one-half ($\sim$250 pc), for example, the filling factor would then increase to $\sim$15%.

Requiring $n \sim 7$ cm^{-3} means pressures range from 3×10^4 to 6×10^4 cm^{-3} K. If the phases of the ISM are in pressure equilibrium, such high pressures for the WNM are not consistent with other measurements of the WNM in the Galaxy. Maintaining pressure equilibrium requires $n \sim$ 1–2 cm^{-3} in the WNM in NGC 6946—not a possible solution if all of the [C II] emission originates in the WNM. If we require pressure equilibrium, however, the expected [C II] intensity in this case (2×10^{-6} ergs s^{-1} cm^{-2} sr^{-1}) would comprise only 13% of what we observed provided all of the observed H I column density was in the WNM.

Figure 6 gives possible solutions of temperatures and densities for a range of ratios of observed I_{C+}/N(H I) for X_e ranging from 10^{-4} to 10^{-1}. Included in the solutions are both H and electron impact excitation of [C II]. The ratio of I_{C+} to N(H I) observed in the extended component of NGC 6946 is shown with a horizontal line.

4.2.3. *Diffuse* H II *Regions*

[C II] emission may also originate from the fully ionized interstellar medium. In the Galaxy the diffuse ionized medium was first revealed through its radio continuum emission (Westerhout 1958) and recently more firmly established through pulsar dispersion measures and faint diffuse optical line emission (Reynolds 1988, 1989, 1991). This diffuse ionized medium extends $\sim$13 kpc from the Galactic center and has a scale height of at least about 1 kpc. The diffuse warm ionized medium (WIM) is a collection of extended low-density (ELD) H II regions, with electron temperatures (T_e) $\sim$ 8000 K and densities $n_e \leq 1$ cm^{-3} (Mezger 1978; Kulkarni & Heiles 1987; Reynolds 1991) assumed to be in pressure equilibrium with other atomic phases. We use the 2.8 cm (10.7 GHz) radio continuum data of Klein et al. (1982) to place upper limits on the contribution of the ionized gas to the observed [C II] emission in the extended component. When the 2.8 cm emission is separated into thermal and nonthermal emission in NGC 6946 (Klein et al. 1982), the thermal contribution to the measured brightness (T_b) in the region to the southeast is no more than 1.0–1.5 mK corrected for our 55″ beam ($\sim$20% of total 2.8 cm emission). The observed flux of free-free emission from ionized gas at frequency, ν, is given for optically thin cases by (Spitzer 1978)

$$S_\nu = 2kT_b/\lambda^2 = 5.44 \times 10^{-39} g_{\rm ff} Z_i^2 T_e^{-1/2} e^{-h\nu/kT} (n_e^2 l) , \quad (6)$$

where S_ν is in units of ergs s^{-1} cm^{-3} Hz^{-1} sr^{-1}, Z_i is the atomic number of the ions which we assume to be only hydrogen, $n_e^2 l$ is the emission measure (EM) along the line-of-sight path length (l), and $g_{\rm ff}$ is the Gaunt factor which is expressed as

$$g_{\rm ff} = 9.77[1.0 + 0.130 \log (T_e^{3/2}/\nu)] . \quad (7)$$

Assuming $T_e = 8000$ K for the 2.8 cm observations gives $g_{\rm ff} \sim 5$. Applying equation (6) directly to the 10.7 GHz data in the extended [C II] region, we derive a range for the EM in the extended [C II] region of 42–62 cm^{-6} pc. The expected [C II] intensity originating from ionized regions, I_{C+}(ionized), can be expressed as

$$I_{C+}(\text{ionized}) = \frac{h\nu}{4\pi} \frac{A}{n_{\rm crit}} \left\{ \frac{g_u/g_l}{1 + [(g_u/g_l) + 1](n_e/n_{\rm crit})} \right\} X_{C+} \, \text{EM} . \quad (8)$$

A is the spontaneous emission coefficient for the $^2P_{3/2}$–$^2P_{1/2}$ transition, 2.36×10^{-6} s^{-1}, the ratio of statistical weights in the upper and lower levels is $g_u/g_l = 2$, and X_{C+} is the abundance of C^+ relative to hydrogen. For $n_{\rm crit} \sim 35$ cm^{-3} at $T \sim 8000$ K (Hayes & Nussbaumer 1984), the ratio of expected [C II] emission from ionized regions to the intensity we observe in the extended [C II] region ($I_{C+} = 1.5 \times 10^{-5}$ ergs

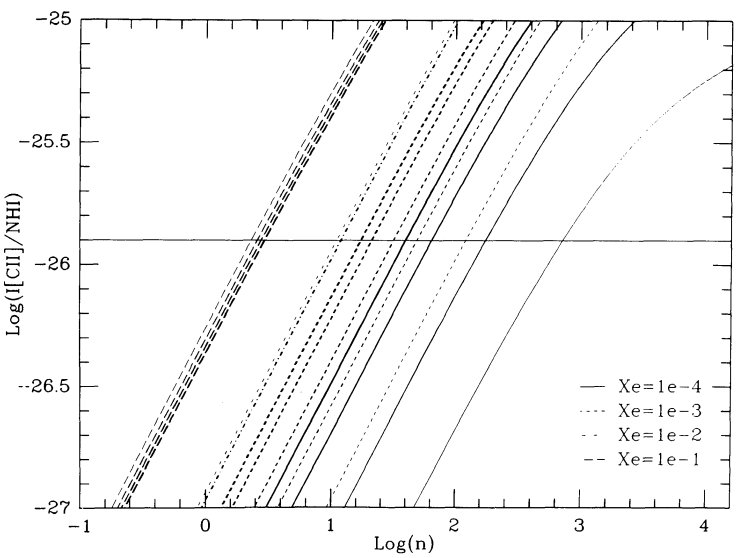

FIG. 6.—Solutions for ratios of observed [C II] intensity and H I column density for various temperatures and X_e. The plotted lines are constant temperatures shown increasing in line width for increasing values of temperature. $X_e = 10^{-4}$ (*solid line*) is plotted for temperatures of 30, 50, 100, and 200 K; $X_e = 10^{-3}$ (*short dash*) is for 50, 100, 200, 1000, 8000 K; $X_e = 10^{-2}$ (*dot-dash*) is for 4000–10,000 K; $X_e = 10^{-1}$ (*long dash*) is for 4000–10,000 K. The horizontal line represents our observed ratio for the extended [C II] component.

s^{-1} cm^{-2} sr^{-1}) is given as

$$\frac{I_{C^+}(\text{ionized})}{I_{C^+}} = (0.48 \pm 0.1)\left(\frac{1}{1 + 3n_e/n_{\text{crit}}}\right)\left(\frac{X_{C^+}}{3.3 \times 10^{-4}}\right), \quad (9)$$

where the uncertainty in the parentheses is due to the range of emission measure values. If we assume (1) a solar fractional abundance of carbon (3.3×10^{-4}), (2) all of the carbon is in the form of C^+ in these regions, and (3) $n_e \ll n_{\text{crit}}$, we find that at most 48% ± 10% of our measured [C II] emission in the extended component can originate from the ionized regions. If we assume pressure equilibrium for the WIM, $n_e = 0.5$ cm^{-3} if the pressure is ~8000 cm^{-3} K. If some of the carbon has condensed onto grains, the WIM would result in a smaller contribution to the [C II] intensity. We also point out that the extended region seen in [C II] to the southeast in NGC 6946 is mostly devoid of observed radio continuum. We conclude that the ionized gas of the ISM can be a significant source of the extended [C II] emission in NGC 6946.

The estimated fraction of [C II] emission from diffuse H II regions in NGC 6946 is in good agreement with the percentage of the Galactic [C II] line luminosity expected from the ionized regions (Stacey 1989; see also Stacey 1985). The recent results of Shibai et al. (1991), Wright et al. (1991), and Gry, Lequeux, & Boulanger (1992) support these predictions.

A possible way of distinguishing the [C II] line emission from atomic neutral and ionized gas regions is through observations of the 205 μm [N II] line since [N II] only arises from ionized regions, while [C II] can be found in both neutral and ionized gas. In ionized gas at low densities the [C II] line emission is 10 times greater than the 205 μm [N II] line.

4.2.3. *Heating of the* H I *Medium*

The [C II] cooling rate per hydrogen atom in the H I medium of NGC 6946 is

$$A_{[C\,II]} = 4\pi I_{C^+}/N(\text{H I}) = 1.7 \times 10^{-25} \quad [\text{ergs s}^{-1}\ \text{atom}^{-1}]\ . \quad (10)$$

This is similar to the [C II] cooling rate estimated in the local diffuse medium in our Galaxy (~10^{-25} ergs s^{-1} $atom^{-1}$) by Pottasch et al. (1979) based on UV absorption measurements. For photoelectric heating (Draine 1978) by far-ultraviolet energy flux χ, the heating rate per hydrogen atom is

$$\Gamma_{pe} = 4 \times 10^{-26}(\chi/\chi_0) \quad [\text{ergs s}^{-1}\ \text{atom}^{-1}]\ . \quad (11)$$

Setting equations (10) and (11) equal requires $\chi \approx 5 \times \chi_0$. Using a combined 100 and 160 μm FIR intensity (~2.4×10^{-3} ergs s^{-1} cm^{-2} s^{-1}; Engargiola 1991), we infer an average energy density of the far-infrared radiation field of about $12\chi_0$ in the southeastern region of the extended component. In order to explain the observed heating and cooling rates of equations (10) and (11), about 40% of the total far-infrared energy density must have originally been emitted in the ultraviolet spectral region. This fraction is typical of the radiation field of OB stars (see Wolfire et al. 1990). We conclude that photoelectric heating by UV photons of the general diffuse radiation field in the disk of NGC 6946 can plausibly account for the observed [C II] cooling in the neutral atomic interstellar medium.

5. ORIGIN OF THE H I EMISSION IN THE SPIRAL ARMS

Another important issue is the origin of the 21 cm H I emission toward the spiral arms seen as local maxima in the cut of Figure 2. The beam-averaged H I column density $\langle N(\text{H I})\rangle$ in photodissociation regions is given by the expression (Sternberg & Dalgarno 1989)

$$\langle N(\text{H I})\rangle = 5 \times 10^{20} \ln[90(\chi/\chi_0)/n_{\text{H}} + 1]\Phi_{\text{FIR}}\ \text{cm}^{-2}\ . \quad (12)$$

For the spiral arms in NGC 6946, PDR solutions exist for $n_{\text{H}} \sim 2 \times 10^5$ cm^{-3} ($\chi \sim 2 \times 10^3\chi_0$) and $n_{\text{H}} \sim 3 \times 10^2$ cm^{-3} ($\chi \sim 320\chi_0$) (Table 2). The beam-averaged H I column densities are therefore 2.6×10^{18} and 1.7×10^{20} cm^{-2} for the high- and low-density solutions, respectively. From 21 cm observations the beam-averaged H I column densities associated with the spiral arm component are 2.0–2.5 × 10^{20} cm^{-2} (Fig. 1*d*; Carignan et al. 1990; Tacconi & Young 1986). Therefore for high-density PDR solution, only a minor fraction of the H I in the spiral arms of NGC 6946 is the result of UV radiation from OB stars photodissociating molecular clouds. However, for the (more likely) low-density solution, the column density of the H I in such PDRs is 70%–80% of the observed H I column density. This result supports the conclusions of Tilanus & Allen (1989), Allen, Atherton, & Tilanus (1986), and Vogel, Kulkarni, & Scoville (1988) that the H I ridges observed downstream of the spiral arms in M51 and M83 are the product of photodissociation of molecular clouds by nearby OB stars. Stacey et al. (1991) arrived at a similar conclusion for starburst nuclei: much of the atomic medium is the product—not the precursor—of star formation.

6. CONCLUSIONS

We present the first large-scale well-sampled map (23 × 17 kpc) of the strong far-infrared cooling line [C II] in an external galaxy. We find that the line emission in NGC 6946 is present in three spatially distinct components: nucleus, spiral arms, and extended region. Most of the [C II] luminosity in NGC 6946 comes from an extended emission region, seen out to a radius of at least 12 kpc. We analyze the [C II] emission in light of possible origins from photo-dominated regions, atomic neutral gas, and the diffuse H II regions. Our specific conclusions are the following:

1. The 1′ nuclear component has a line luminosity of 1.5×10^7 $L_\odot$ and contributes 0.15% of the galaxy's total far-infrared luminosity. The hydrogen mass associated with the [C II] emission is estimated to be 2.8×10^7 $M_\odot$, and the density determined from PDR models is high ($n > 10^5$ cm^{-3}). Use of the [C II] emission as an indicator of star formation leads to the conclusion that the nucleus of NGC 6946 is not particularly active at the present time.

2. The spiral arms are clearly seen in [C II] emission, the most prominent being the east/northeast arms. The spiral arm component is most likely associated with moderate density, photodissociation surfaces of molecular clouds. The H I emission associated with the spiral arms may also predominantly come from these PDRs if the cloud density is 10^3 cm^{-3}.

3. An extended component of [C II] emission exists past the molecular extent of the galaxy. It is present to at least the full dimensions of the map. This is the first detection of diffuse [C II] emission in an external galaxy. We interpret this component as arising from a mixture of neutral and atomic clouds. The major of the extended [C II] emission probably originates in cloudy, cold ($T \sim 100$ K) H I clouds with pressures between 6×10^3 and 1×10^4 cm^{-3} K. Diffuse ionized gas could contribute up to ~50% of the observed [C II] emission if we assume pressure equilibrium among the atomic phases.

Warm ($T \sim 8000$ K) neutral gas does not explain a significant fraction of the [C II] emission unless it is clumped with a filling factor of less than 0.1 or if it has an ionization fraction exceeding 10%. The physical parameters of the atomic medium of NGC 6946 are quite similar to those inferred for our own Galaxy.

We are grateful to the staff of the Kuiper Airborne Observatory for their support. We thank L. Tacconi for providing us with H I data and A. Harris, C. Heiles, A. Sternberg, and L. Tacconi for helpful discussions. This research was supported, in part, by NASA grant NAG-2-208.

REFERENCES

Allen, R. J., Atherton, P. D., & Tilanus, R. P. 1986, Nature, 319, 296
Ball, R., Sargent, A. I., Scoville, N. Z., Lo, K. Y., & Scott, S. L. 1985, ApJ, 298, L21
Bloemen, H. 1989, ARA&A, 27, 469
Bonnarel, F., Boulesteix, J., & Marcelin, M. 1986, A&AS, 66, 149
Carignan, C., Charbonneau, P., Boulanger, F., & Viallefond, F. 1990, A&A, 234, 43
Casoli, F., Clausset, F., Viallefond, F., Combes, F., & Boulanger, F. 1990, in The Interstellar Medium in External Galaxies, ed. D. J. Hollenbach & H. A. Thronson (NASA CP-3084), 273
Cooksy, A. L., Blake, G. A., & Saykally, R. J. 1986, ApJ, 305, L89
Crawford, M. K., Genzel, R., Townes, C. H., & Watson, D. M. 1985, ApJ, 291, 755
Dalgarno, A., & McCray, R. 1972, ARA&A, 10, 375
DeGioia-Eastwood, K., Grasdalen, G. L., Strom, S. E., & Strom, K. M. 1984, ApJ, 278, 564
Dickey, J. M., & Lockman, F. J. 1990, ARA&A, 28, 215
Draine, B. T. 1978, ApJS, 36, 595
Engargiola, G. 1991, ApJS, 76, 875
Flower, D. R., & Launay, J. M. 1977, J. Phys. B., 10, 3673
Geis, N. 1991, Ph.D. thesis, Ludwig-Maximillians-Univ., Munich
Genzel, R., Harris, A. I., & Stutzki, J. 1989, in Proc. 22d ESLAB Symp.: Infrared Spectroscopy in Astronomy, ed. B. H. Kaldeich (SA SP-290), 115
Gry, C., Lequex, J., & Boulanger, F. 1992, A&A, submitted
Hayes, M. A., & Nussbaumer, H. 1984, A&A, 134, 193
Heiles, C. 1988, Lecture Notes in Physics, Vol. 306, The Outer Galaxy, ed. L. Blitz & F. J. Lockman (Berlin: Springer)
Ishizuki, S., Kawabe, R., Ishiguro, M., Okumura, S. K., Morita, K.-I., Chikada, Y., Kasuga, T., & Doi, M. 1990, ApJ, 335, 436
Jenkins, E. B., Jura, M., & Lowenstein, M. 1983, ApJ, 270, 88
Klein, U., Beck, R., Buczilowski, U. R., & Wielebinski, R. 1982, A&A, 108, 176
Klein, U., & Emerson, D. T. 1981, A&A, 94, 29
Kulkarni, S., & Heiles, C. 1987, in Interstellar Processes, ed. D. J. Hollenbach & H. A. Thronson (Dordrecht: Reidel), 87
———. 1988, Galactic and Extragalactic Radio Astronomy, ed. G. Verschuur & K. Kellerman (Berlin: Springer), 95
Launay, J. M., & Roueff, E. 1977, J. Phys. B, 10, 879
Lugten, J. B., Watson, D. M., Crawford, M. K., & Townes, C. H. 1986, ApJ, 306, 691
Mezger, P. G. 1978, A&A, 70, 565
Poglitsch, A., et al. 1990, in Proc. 29th Liège Internat. Astrophysics, ed. B. H. Kaldeich (ESA SP-314), 149
Poglitsch, A., et al. 1991, Internat. J. IR MM Waves, 12, 859
Pottasch, S. R., Wesselius, P. R., & van Duinen, R. J. 1979, A&A, 74, L15
Reynolds, R. J. 1988, ApJ, 333, 341
———. 1989, ApJ, 345, 811
———. 1991, in IAU Symp. 144, The Interstellar Disk-Halo Connection in Galaxies, ed. S. Boyer & C. Leinert (Dordrecht: Kluwer), 157
Rogstad, D. H., Shostak, G. S., & Rots, A. H. 1973, A&A, 22, 111
Russell, R. W., Melnick, G. J., Smyers, S. D., Kurtz, N. T., Gosnell, T. R., Harwit, M., & Werner, M. W. 1981, ApJ, 250, L35
Sandage, A., & Tammann, G. A. 1974, ApJ, 194, 559
Shibai, H., et al. 1991, ApJ, 374, 522
Smith, J., Harper, D. A., & Lowenstein, R. F. 1984, in Proc. Airborne Astronomy Symp., ed. H. A. Thronson, Jr., & E. F. Erickson (NASA CP-2353), 277
Sofue, Y., Doi, M., Ishizuki, S., Nakai, N., & Handa, T. 1988, PASJ, 40, 511
Spitzer, L. 1978, Physical Processes in the Interstellar Medium (New York: Wiley)
Stacey, G. J. 1985, Ph.D. thesis, Cornell Univ.
———. 1989, in Proc. 22 Elsab Symp., ed. B. H. Kaldeich (ESA SP-290)
Stacey, G. J., Beeman, J. W., Haller, E. E., Geis, N., Poglitsch, A., & Rumitz, M. 1992, Internat. J. IR MM Waves, 13, 1689
Stacey, G. J., Geis, N., Genzel, R., Jackson, J., Poglitsch, A., & Townes, C. H. 1990, in Proc. 29th Liège International Astrophysics, ed. B. H. Kaldeich (ESA SP-314), 85
Stacey, G. J., Geis, N., Genzel, R., Lugten, J. B., Poglitsch, A., Sternberg, A., & Townes, C. H. 1991, ApJ, 373, 423
Stacey, G. J., Viscuso, P. J., Fuller, C. E., & Kurtz, N. T. 1985, ApJ, 289, 803
Sternberg, A., & Dalgarno, A. 1989, ApJ, 338, 197
Tacconi, L. J., & Young, J. S. 1986, ApJ, 308, 600
———. 1989, ApJS, 71, 455
Tacconi, L., Tacconi-Garman, L., & Xie, S. 1993, in preparation
Tielens, A. G. G. M., & Hollenbach, D. 1985, ApJ, 291, 722
Tilanus, R. P. J., & Allen, R. J. 1989, ApJ, 339, L57
van der Kruit, P. C., Allen, R. J., & Rots, A. H. 1977, A&A, 55, 421
Vogel, S. N., Kulkarni, S. R., & Scoville, N. Z. 1988, Nature, 334, 402
Weliachew, L., Casoli, F., & Combes, F. 1988, A&A, 199, 29
Westerhout, G. 1958, A&A, 67, 437
Wild, W. 1991, Ph.D. thesis, Ludwig-Maximillians-Univ., Munich
Wolfire, M., Hollenbach, D. J., & Tielens, A. G. G. M. 1990, ApJ, 358, 116
Wright, E. L., et al. 1991, ApJ, 381, 200